RELATIVE INTENSITIES OF GAMMA RAYS IN BETA DECAY OF W 187

by

NAI CHENG CHAO

Diploma, Taiwan Provincial Taipei Institute of Technology, 1962

A MASTER'S THESIS

submitted in partial fulfillment of the

requirements for the degree

MASTER OF SCIENCE

Department of Physics

KANSAS STATE UNIVERSITY
Manhattan, Kansas

1967

Approved by:

C. E. Mandeville
Major Professor

TABLE OF CONTENTS

INTRODUCTION

The purpose of this experiment was to measure, with better accuracy than presently available, the relative intensities of gamma rays in the beta decay of W^{187}, using a lithium-drifted germanium detector. Determination of accurate relative intensities of gamma rays is the first important step in constructing an energy level scheme of Re^{187}.

The beta decay of W^{187} (T 1/2 = 24 h) and the energy level scheme of Re^{187} have been studied by many groups of researchers (1-5). Several methods using magnetic beta-ray spectrometers and NaI(Tl) scintillation spectrometers have been used by them to determine the relative intensities of gamma-rays in the W^{187} decay. Although magnetic beta-ray spectrometers have good energy resolution, assignment of energy and intensity to weak gamma rays is rendered uncertain because of the overlapping of electron lines originating in different shells and subshells. Scintillation spectrometers of NaI(Tl) have poor energy resolution so that if full energy peaks of relatively weak gamma rays are in the near vicinity of those of stronger gamma rays, difficulties are encountered in determining the relative intensities accurately. The most suitable method is by using a Ge(Li) detector, which has good energy resolution. A Ge(Li) detector with its high energy resolution incorporated with a multi-channel analyzer provides an accurate method for determining relative intensities of gamma rays.

Recently a study of W^{187} decay using a Ge(Li) detector of 1.3 cm^2 active area and 4 mm depletion depth has been done by Sébille (6). Plate I shows the decay scheme proposed by Gallagher (3) and extended by Sébille (6).

One disadvantage of a Ge(Li) detector is its poor detection efficiency. However, this can be compensated for by using a more active source or a larger

EXPLANATION OF PLATE I

The disintegration scheme of the beta decay of W^{187} based on the results of Gallagher and Sébille.

PLATE I

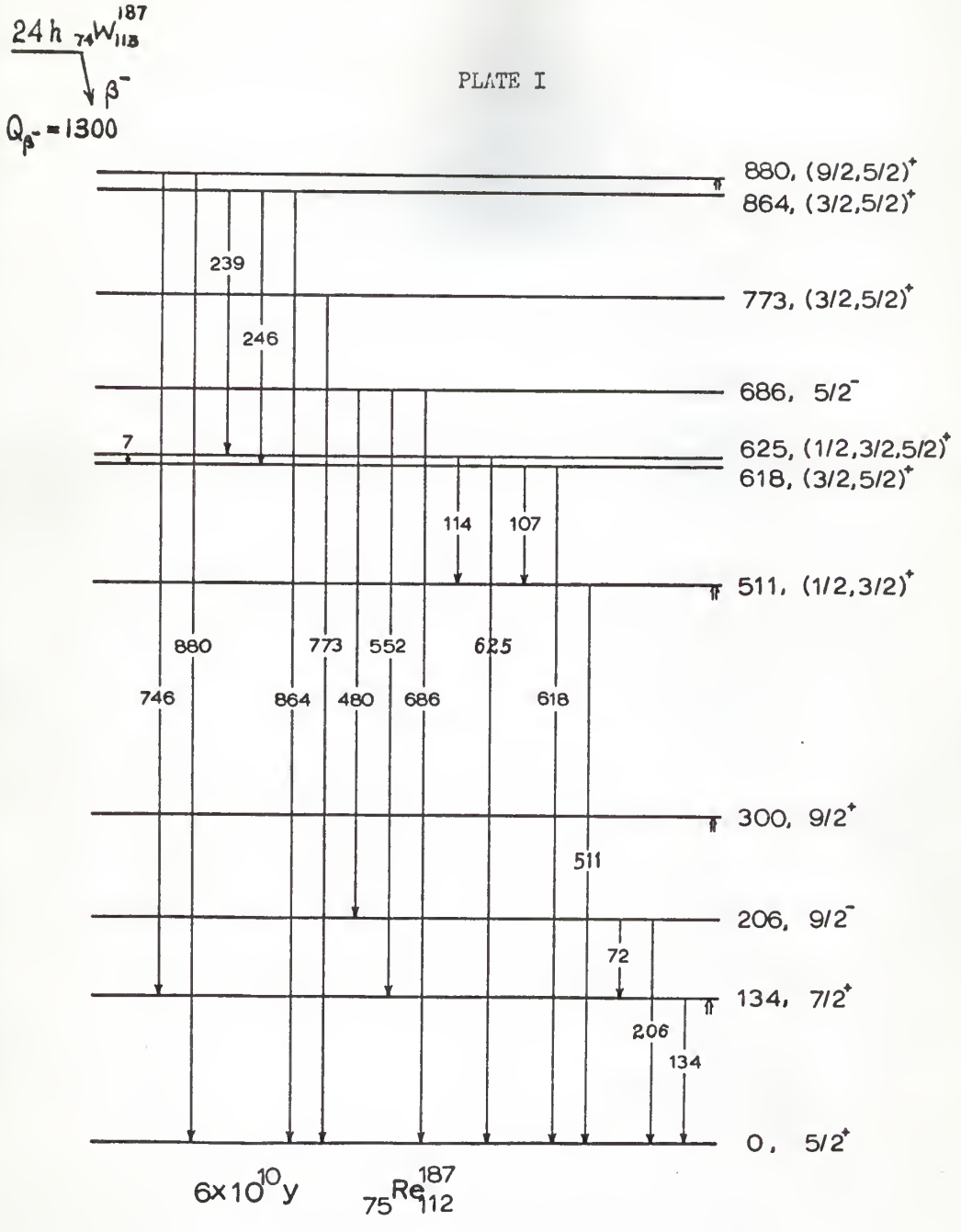
24 h 74W187 115
β⁻
Qβ⁻ = 1300
880, (9/2,5/2)⁺
864, (3/2,5/2)⁺
773, (3/2,5/2)⁺
686, 5/2⁻
625, (1/2,3/2,5/2)⁺
618, (3/2,5/2)⁺
511, (1/2,3/2)⁺
300, 9/2⁺
206, 9/2⁻
134, 7/2⁺
0, 5/2⁺
239
246
7
114
107
880
773
552
625
746
864
480
686
618
511
72
206
134
6x10¹⁰y
75Re187 112

detector volume. In this experiment, a Ge(Li) detector with an active area of 8 cm^2 and a depletion depth of 5 mm was used. Thus, a better result was expected, as compared to the recent work of Sébille (6).

INTERACTION OF GAMMA-RAYS WITH THE Ge(Li) DETECTOR

Gamma-rays are electromagnetic radiations associated with the nuclear transition from excited energy states to one of smaller excitation energy or to the ground state. Since the nucleus has discrete energy levels, the γ-ray quanta emitted have a definite energy which is equal to the difference between the two energy levels,

$$h\nu = E_i - E_f$$

where h is Planck's constant; ν is the frequency of the radiation; E_i is the energy of the initial energy level, and E_f is the energy of the final energy level of the nucleus.

The characteristic of γ-ray interaction with any matter, viz. Ge(Li) detector, is that γ-ray photons are absorbed or scattered individually in a single event. Thus, the number of photons eliminated from the incident beam, ΔN, is proportional to the thickness traversed, Δx, and to the number of incident photons, i. e.

$$\Delta N = -\mu N \Delta x,$$

where μ is the absorption coefficient. This leads to the exponential attenuation. The equation on integration becomes

$$N = N_o e^{-\mu x}$$

where N_o is the number of incident photons.

The attenuation coefficient, μ, is the sum of partial attenuation coefficients of independent modes of interaction.

For γ-ray energies between 10 keV to about 5 MeV, the wavelengths of the γ-ray are about 1.2×10^{-8} cm to 2.5×10^{-11} cm. These are less than atomic dimensions and much greater than nuclear dimensions. Thus, the interaction will mainly be outside the nucleus; that is, γ-ray photons of these

energies interact only with the atomic electrons or the nuclear electric field, resulting in the following most important effects:

(a) Photoelectric effect

For γ-ray energies below 100 keV and greater than the electron binding energy of the atom which interacts with the γ-ray photon, the predominant mode of interaction is the photoelectric process. In this process the incident photon is completely absorbed by one of the bound electron of an atom.

Consider the case of a free electron initially at rest which absorbs an incident photon. Before interaction, the system consists of a photon of energy $h\nu$, and momentum $h\nu/c$. After interaction, the photon disappears, the system then consists only of the electron with kinetic energy $T = h\nu$, so as to conserve energy. However, the momentum of the electron with kinetic energy T would be $p = \frac{1}{c}\sqrt{T(T + 2mc^2)}$ which cannot be equal to T/c or $h\nu/c$ the momentum of the initial system. Therefore, an incident photon cannot be completely absorbed by a free electron. It is clear that the incident photon should interact with the whole atom in order to be absorbed. Thus, the total absorption can only take place if the electron is initially bound in an atom. Momentum is then conserved by the recoil of the residual atom. This also explains the fact that the probability of photoelectric absorption increases with the tightness of binding of the electron, so that at energies greater than the K- and L-shells, the absorption due to outer shells is negligible. Actually, about 80 per cent of the photoelectrons are ejected from the K-shell.

From the theory of photoelectric effect, the photoelectric absorption coefficient can be expressed as (7)

$$\sigma_{photo} \propto N Z^5 E_\gamma^{-3.5} \text{ cm}^{-1}$$

where N is the number of absorber atoms per cm^3 and Z is the atomic number of

the absorber.

This expression shows σ_{photo} increases very rapidly with atomic number and decreases very rapidly with photon energy. The dependence on Z can be understood by the dependence of binding energy on Z. Also, electrons are relatively more tightly bound for low energy photons. Thus, the probability of photoelectric absorption increases as the energy of the γ-rays decreases.

Because the nuclear mass is very large compared with that of the electron, the energy taken by the recoiling nucleus is negligible. Therefore, the ejected photoelectron has kinetic energy

$$T = h\nu - B_e$$

where B_e is the binding energy of the ejected electron.

The result of this process leaves a vacancy in the shell from which the photoelectron was ejected. The atom then immediately emits characteristic X-rays or Auger electrons. The emitted X-rays are generally absorbed by a second photoelectric effect and the total energy of the incident photon is absorbed by the matter.

(b) Compton effect

For the energy range between 0.1 MeV and 10 MeV, the energies of the incident photons are much higher than the binding energies of the atomic electrons. The loosely bound electrons can be considered as free electrons. Since an incident photon cannot be absorbed by a free electron, it will be scattered with a lower energy, the remainder of the energy being taken by the recoil electron. This inelastic collision of a photon with a free electron is known as the Compton effect.

Applying the conservation of energy and momentum, the energies of the scattered photon and the recoil electron are given by the following equations:

$$E'_\gamma = \frac{E_\gamma}{1 + \frac{E_\gamma}{mc^2}(1 - \cos\theta)}$$

$$E_e = E_\gamma - E'_\gamma = \frac{E_\gamma}{1 + \frac{mc^2}{E_\gamma (1 - \cos\theta)}}$$

where E_γ is the energy of the incident photon, E'_γ is the energy of the scattered photon and θ is the angle between the direction of the primary and scattered photons. Since the angle θ can vary from 0° to 180°, the corresponding energy of the scattered Compton electron, varies from zero energy to maximum energy, $(E_e)_{max}$,

$$(E_e)_{max} = \frac{E_\gamma}{1 + \frac{mc^2}{2E_\gamma}}$$

$$\doteq E_\gamma - \frac{mc^2}{2}$$

when E_γ is very large compared with mc^2, the backscattered photons have an energy of $mc^2/2$ which is equal to 0.257 MeV.

The Compton scattering coefficient, as given by Klein and Nishna, can be expressed as (7)

$$\sigma_{Compton} \propto NZE_\gamma^{-1}\left[\ln\left(\frac{2E_\gamma}{mc^2}\right) + 1/2\right]^{-1} \text{ cm}^{-1}$$

where N, Z and E_γ are as previously defined. This shows the Compton scattering coefficient increases linearly with Z and decreases approximately linearly with γ-ray energy.

Comparing photoelectric absorption coefficient with Compton scattering coefficient, it is seen that the ratio $\frac{\sigma \text{ photo}}{\sigma \text{ Compton}}$ goes as Z^4 and $E_\gamma^{-2.5}$. Thus for high Z absorber, the photoelectric absorption is much more probable than Compton scattering. On the other hand, the photoelectric absorption

decreases more rapidly than Compton scattering as the γ-ray energy increases. Thus, for each element, the photoelectric effect predominates below a certain energy, and above this energy the Compton effect is predominant.

(c) Pair Production

For γ-ray energy greater than 1.02 MeV, another total absorption effect occurs. This phenomenon is the disappearance of a photon resulting in the formation of an electron-position pair.

Pair production cannot take place in free space, because it can be shown that the disappearance of a photon, followed by the appearance of an electron and positron, cannot conserve both total relativistic energy and momentum. Therefore, it is necessary for the process to take place in the Coulomb field of an atom because there can be interactions between the pair of charged particles and the nucleus. These interactions allow the massive nucleus to absorb the required momentum and conserve momentum without affecting the energy balance.

The production of electron-positron pairs can be explained by Dirac's relativistic theory of electrons. In this theory the allowed values of total relativistic energy E for a free electron are

$$E = \pm\sqrt{c^2p^2 + (m_oc^2)^2} ,$$

where m_o is the electron rest mass. The negative energy levels are normally occupied at all points in space. An incident photon with energy greater than $2mc^2$ can excite the negative energy state electron to a positive energy state, thus producing an electron and a hole, which is the positron.

After the positron has slowed down by collision with the atoms, it will annihilate with an electron, resulting in the creation of two photons each with an energy 0.511 MeV.

The pair production results in total energy absorption of the γ-ray.

The absorption coefficient is proportional to Z^2 and increases with increasing γ-ray energy.

(d) Analysis of γ-ray Spectra (8)

In the study of γ-radiations, NaI(Tl) and Ge(Li) detectors are often used, and commercially produced multichannel analyzers are employed to accumulate the pulse spectra.

In these spectra, usually appear photopeaks and several continuous Compton distributions.

The photopeak corresponding to total absorption of γ-ray energy is the most significant characteristic of a spectrum. The energy of such a peak and its intensity are used to determine the energy and intensity of γ-rays producing a given pulse-height distribution. The full width at half the maximum height of this peak is a measure of the energy resolution of the detector.

The photopeak results not only from the photoelectric effect, but also from many multiple events which result in total energy loss. Such multiple events are, for example, Compton scattering followed by a photoevent and pair production, in turn followed by absorption of the two annihilation quanta.

However, if the X-rays produced following a photoelectric interaction escape from the surface of the detector, a peak of smaller intensity will appear on the low energy side of the full-energy peak. This X-ray escape peak can be identified, because it has energy less than the full-energy peak and the energy difference is equal to the K-shell electron binding energy of the detector material.

The Compton distribution results from the absorption of Compton electrons and the scattered photons escape the detector. For the maximum energy of

the Compton electrons the pulse observed is the so called Compton edge. There is also a definite peak superimposed upon the otherwise flat energy distribution of Compton electrons. This peak is the "backscattered peak" and arises from Compton scattering of gamma rays in the walls of the shield surrounding the detector.

For γ-rays the energy of which exceeds the threshold for pair production, the pulse-height distribution becomes more complicated. In addition to the full-energy peak and the Compton distribution, several satellite peaks are superimposed upon the Compton distribution as a result of interaction by the pair production process. The absorption of the total energy of the electron-positron pair gives a full-energy peak at E_γ. However, the annihilation of the positron will create two 0.511 MeV photons within the detector. If both of the annihilation quanta escape detection, then a peak will appear at an energy corresponding to 1.02 MeV less than the full-energy peak and known as the "double escape peak". There may also be a peak at 0.511 MeV less than the full energy peak, which is known as the "single escape peak", corresponding to the detection of one annihilation quantum following the initial absorption due to pair formation. Furthermore, there is also a peak corresponding to 0.511 MeV. This peak is due to the detection of annihilation quanta resulting from pair production external to the detector.

If the detector is shielded for the sake of reducing background radiation, this shield will increase the scattered radiation and produce characteristic X-rays from the surface of the shielding material.

Since an intense high energy beta emitter produces a beta-ray spectrum, an absorbing material must be used to prevent beta particles from reaching the detector. Furthermore, there is usually a bremsstrahlung radiation distribution. This results from the acceleration of beta rays in the field

of the nucleus after they are emitted. A continuous energy distribution of photons results, which decreases rapidly in intensity with increasing energy, to the maximum beta ray energy. The energy loss by bremsstrahlung radiation is proportional to beta ray energy and increases as the square of the atomic number, Z, of the absorbing material.

In the case of the emission of two or more gamma-rays in cascade, there is a finite probability that these gamma-rays will be detected simultaneously. Thus results a "coincident sum peak" which corresponds in energy to the sum of the energies of the coincident gamma-rays. In addition, the accidental time-coincidences between events occurring in the detector, will also result in sum peaks. Consequently, a continuous distribution of pulses extending to approximately twice the amplitude of the full-energy peak will be observed. The intensity of the coincidence sum spectrum for two coincident gamma rays is given by

$$N_{c.s.s.} = N_o \varepsilon_1 \varepsilon_2 W(\theta^o),$$

where N_o is the number of coincident pairs of gamma rays emitted by the source, ε_1 and ε_2 are the efficiencies for the detection of gamma rays 1 and 2, and $W(\theta^o)$ is a factor which takes into account the angular correlation of the two coincident gamma rays. Since N_o will be proportional to the source strength, $N_{c.s.s.}$ will be small for a weaker source.

These effects are the major sources of difficulty in the analysis of the gamma ray spectra and have to be taken into account in the intensity measurements of gamma rays.

EXPERIMENTAL EQUIPMENT

The detection system employed in this experiment consists of (a) the detector-dewar system and, (b) electronics which includes a preamplifier, linear amplifier and pulse-height analyzer. A block diagram exhibiting the connection of the system is shown in Plate II.

(a) The detector-dewar system

The detector used was a lithium-drifted germanium detector manufactured by Isotopes, Inc. It has an active area of 8 cm^2, a depletion depth of 5 mm.

The structure of the Ge(Li) detector is similar to a p-i-n type semiconductor (9). A schematic diagram of the lithium-drifted germanium detector is shown in Plate III. Essentially, the detector is a cylindrical block of germanium crystal. The front region is a heavily doped n^+ material produced by diffusion of lithium into the front surface. The central region is the intrinsic region formed by the lithium-drift process and the back is the original p-type material.

A bias voltage of 440 volts is maintained across the block. Absorption or scattering of gamma-rays within the intrinsic region produces high-speed electrons which lose their energy by creating electron-hole pairs. These electron-hole pairs are collected by the electric field. Thus, electric pulses proportional to the energy absorbed are produced.

In order to reduce the detector leakage current, it was operated at liquid nitrogen temperature (77°K). Also, the detector was kept in vacuum to avoid condensation and contamination of the detector surface.

The detector is mounted on a cold finger in contact with liquid nitrogen. Liquid nitrogen is contained in a dewar which has a capacity of 25 liters. The whole system is kept inside a steel container, forming a detector-dewar

EXPLANATION OF PLATE II

Block diagram showing the apparatus and the electronics used in accumulating singles spectra.

PLATE II

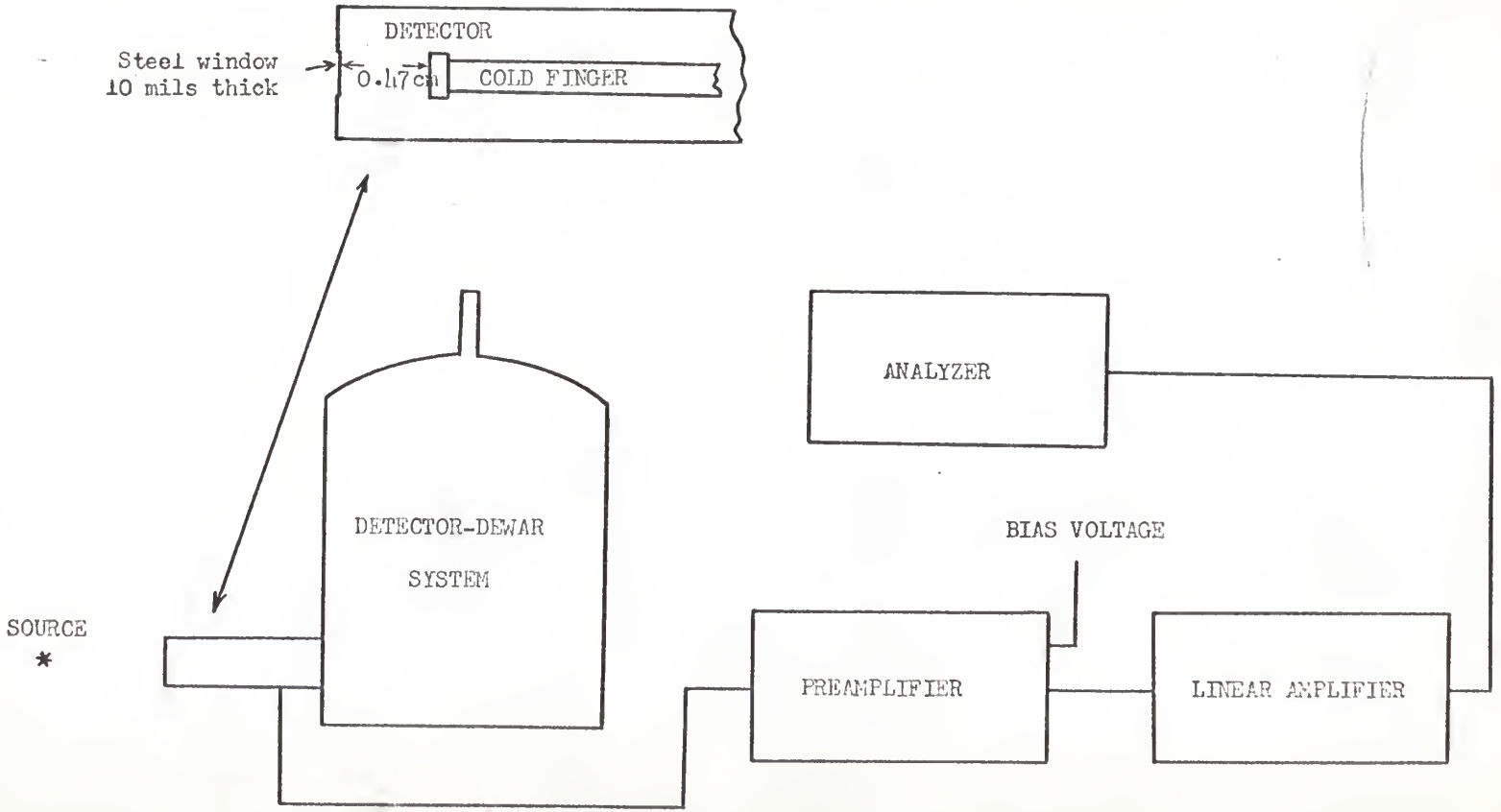
DETECTOR
Steel window
10 mils thick
0.47cm
COLD FINGER
ANALYZER
DETECTOR-DEWAR
SYSTEM
BIAS VOLTAGE
SOURCE
*
PREAMPLIFIER
LINEAR AMPLIFIER

EXPLANATION OF PLATE III

Schematic diagram of a lithium-drifted germanium detector.

Plate III. Schematic diagram of a lithium-drifted germanium detector.

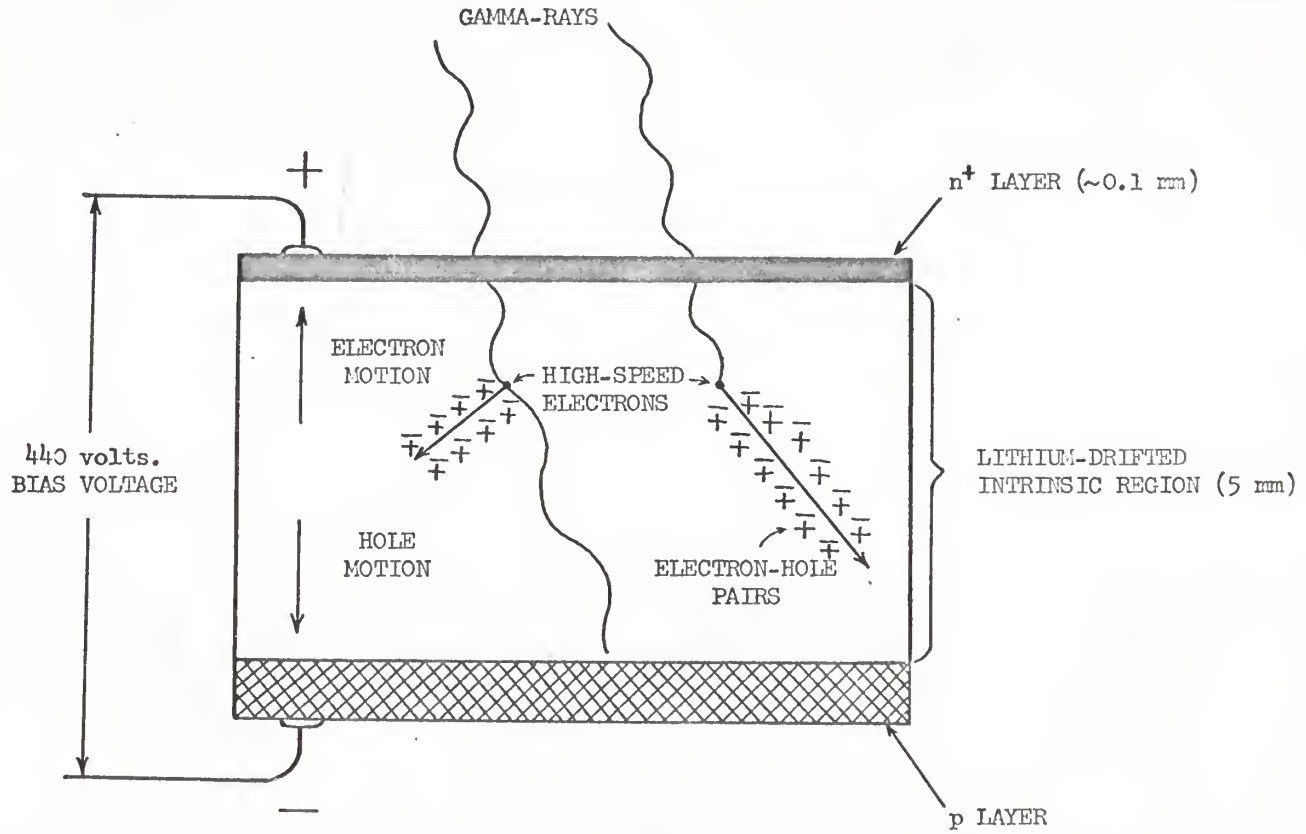

system.

The distance between the detector and steel window is 0.47 cm. The steel window is 10 mils thick which acts unfortunately as an absorber to the incident gamma-rays of low energy.

(b) Electronics

The electrical pulses produced in the Ge(Li) detector were first amplified in a low-noise charge sensitive preamplifier, Tennelec Model TC 130. It has a charge sensitivity of 54 mV/MeV loss in a Ge(Li) detector, according to specifications.

The signal was further amplified by a linear amplifier, Tennelec Model TC 200. This amplifier has RC pulse shaping and a total amplifier gain of 4 to 2048 with an integral nonlinearity of less than 0.05 per cent of rated output as given by the manufacturer's specifications.

The pulses were finally registered according to energy by a pulse-height Analyzer. The analyzer was a 4096-channel Multiparameter Pulse Analyzer with Model 213 Pulse Height Logic Units. This analyzer system has a differential linearity of 2 per cent of full scale, a time stability of less than 0.05 per cent of full scale channel drift per 30 degrees centigrade, and can accept as many as 5 x 10^4 counts per second with no change in drift or linearity, according to specifications.

EXPERIMENTAL PROCEDURE

The W^{187} source was prepared by Oak Ridge National Laboratory. The chemical form of the source is K_2WO_4 in KOH solution. The solution was placed on the adhesive side of "Scotch" tape and allowed to dry. Then the source was sealed with another piece of tape. The diameter of the source was approximately 6-10 mm. A lucite absorber of thickness 5.8 mm was used to absorb beta rays.

The amplifier gains were set to view both low and high energy portion of the spectrum. For high energy spectra, a 0.24 cm thick Cd absorber was used to absorb low energy gamma-rays.

Plates IV and V show typical differential pulse height distributions of gamma-rays from W^{187}, for low and high energy portions, respectively. They have been corrected by subtracting background radiations which were accumulated without the source for the same period of time and for each amplifier gain separately.

The full-energy peaks in a given spectrum are used to determine the relative gamma-ray intensities. However, because of the scattering distribution in a spectrum, the total numbers of gamma-rays entering into the detector should be corrected for peak-to-total ratio and the detector efficiency.

The peak-to-total ratio is defined as the fraction of the total number of events in the pulse-height spectrum which appear in the full-energy peak. This ratio must be determined experimentally for a given geometry because of the large number of multiple processes which occur in the detector. The experimental measurement of the full energy peak-to-total ratio and the calculation of detector efficiency were necessary for the determination of relative gamma-ray intensities.

EXPLANATION OF PLATE IV

The low energy gamma ray spectrum of W^{187}. No extra absorbers were used between the source and the detector.

PLATE IV

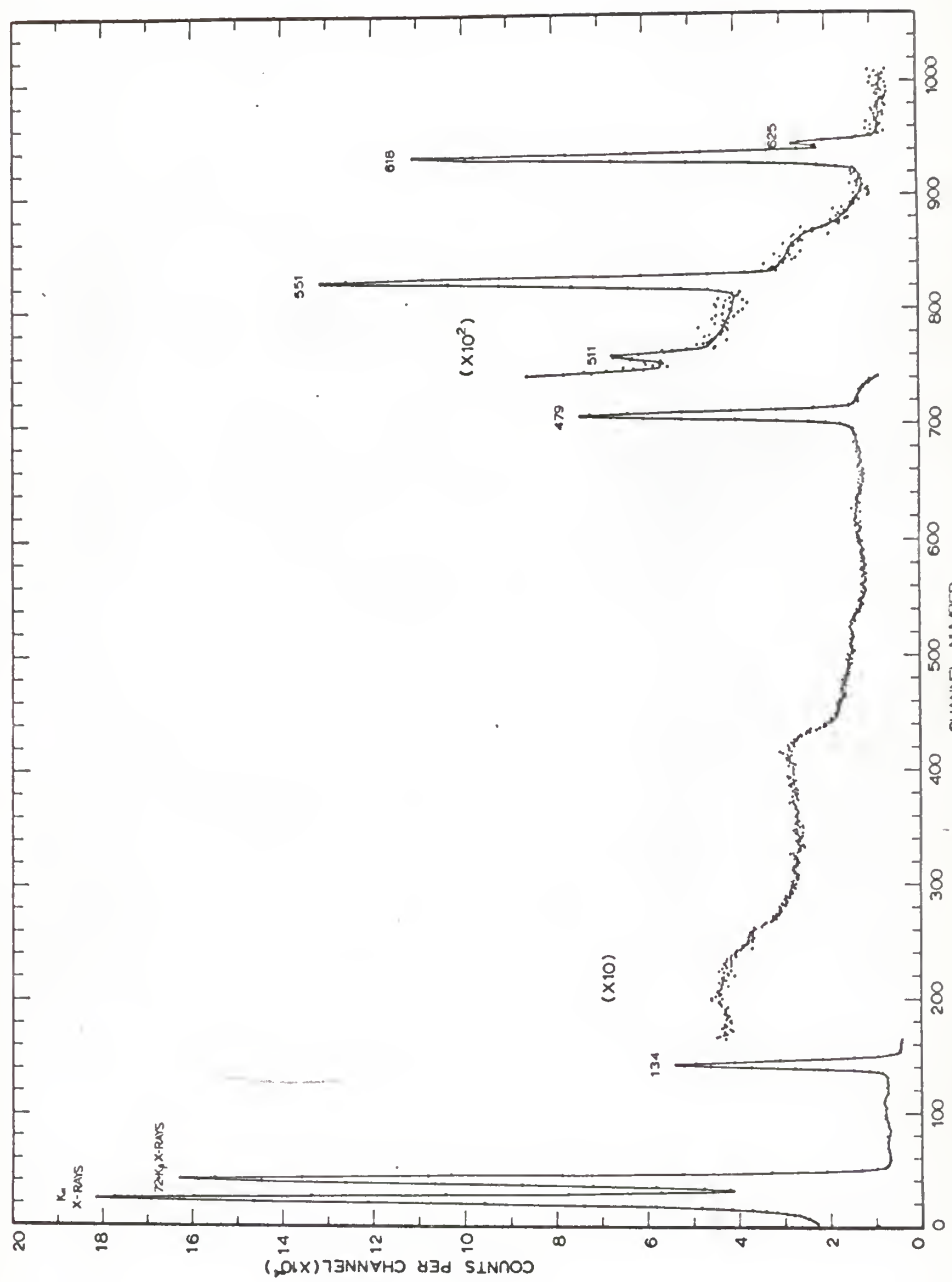
COUNTS PER CHANNEL (X10³)
CHANNEL NUMBER
Kα X-RAYS
72Ky X-RAYS
134
(X10)
479
511
(X10²)
551
618
825

EXPLANATION OF PLATE V

The high energy gamma ray spectrum of W^{187}. A 0.24 cm thick Cd absorber was used to reduce the intensity of the low energy gamma rays.

PLATE V

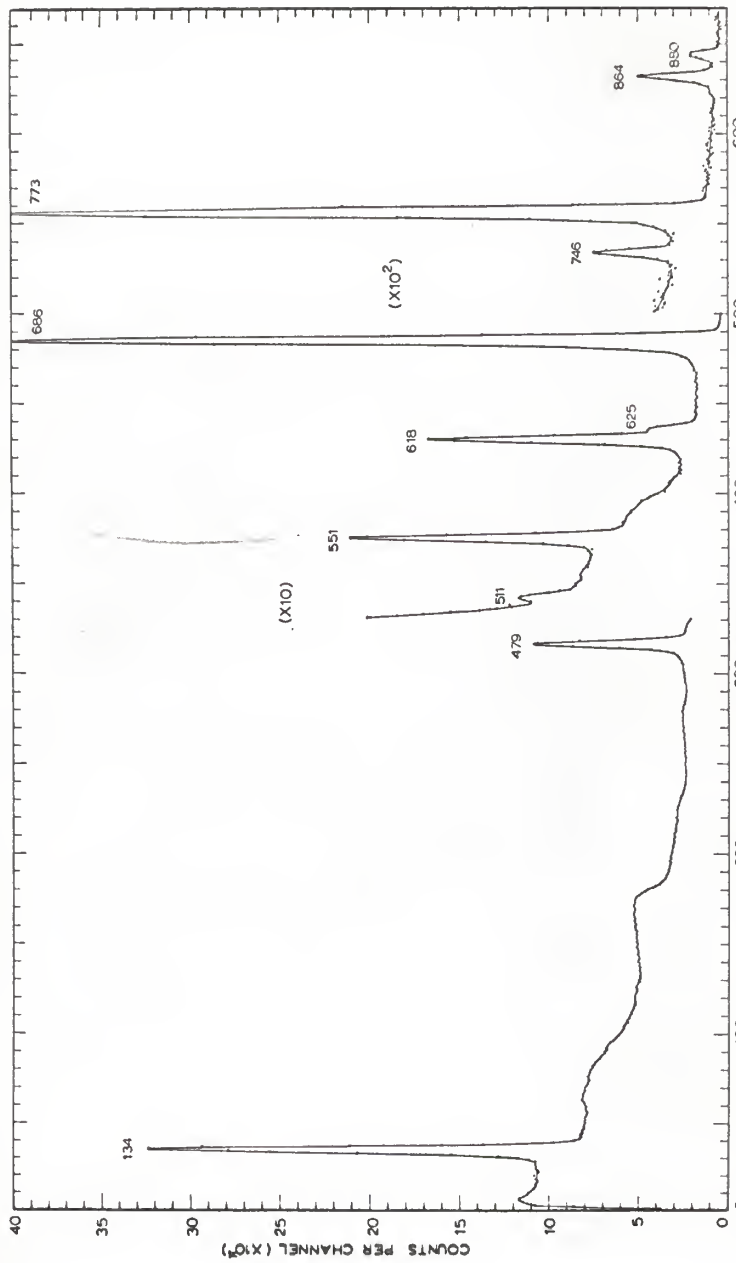
COUNTS PER CHANNEL (X10³)
CHANNEL NUMBER
0
5
10
15
20
25
30
35
40
0
100
200
300
400
500
600
134
479
511
551
618
625
686
746
773
864
880
(X10)
(X10²)

The peak-to-total ratio was calculated from the differential energy spectra of gamma rays emitted in the decay of Na^{22}, Cs^{137}, and Co^{60}. A typical gamma ray spectrum is shown in Plate VI. Cross-sections giving the number of Compton electrons per unit energy of gamma rays are available (10). The cross-section for the gamma ray energies used were found from these tabulated values by log-log interpolation and are given in Table I. The cross-sections for each gamma ray energy were normalized to the experimentally observed spectrum by using an appropriate point near the Compton edge. This point was chosen to minimize other effects appearing at lower energies. This normalization was accomplished by determining the suitable multiplicative factor necessary to make the chosen point coincide with the experimental curve. The other cross-sections were multiplied by this same factor to obtain the theoretical distribution. This theoretical distribution is indicated as a dashed line in Plate VI.

This procedure is shown in Plate VI in the case of Cs^{137}, for which the point chosen for normalization was at $E/E_{max} = 0.8$. This point was chosen to avoid the effect due to backscattered radiation. The normalization factor in this case was found to be 4.845×10^{28}. Using this factor, theoretical Compton distribution for Cs^{137} was calculated and is given in Table II, and is shown as a dashed line in Plate VI.

The total number of counts was found by taking the area under the dashed line from energy zero up to the energy at which the theoretical and actual distributions match and the area under the experimental curve from there to the gamma-ray energy. The number of counts in the full-energy peak was found by taking the area under the peak.

Plate VII shows a plot of peak-to-total ratio versus energy for the detector used in this experiment. The dashed line on this plate indicates

EXPLANATION OF PLATE VI

The gamma ray spectrum of Cs^{137} used to determine the peak-to-total ratio of the detector. The dashed line is the theoretical Compton distribution used in the calculation. The peak-to-total ratio for the 662 keV gamma ray is 0.0507.

PLATE VI

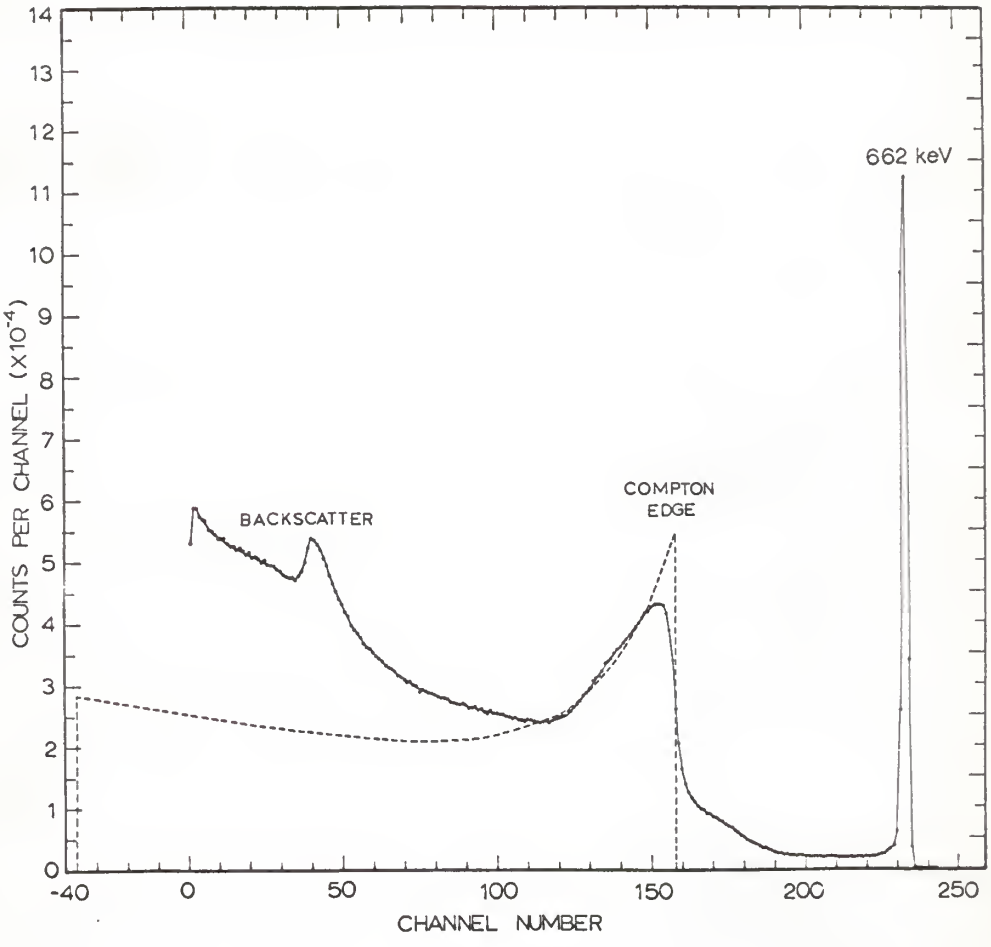
662 keV
COMPTON
EDGE
BACKSCATTER
COUNTS PER CHANNEL (X10⁻⁴)
CHANNEL NUMBER
0
1
2
3
4
5
6
7
8
9
10
11
12
13
14
-40
0
50
100
150
200
250

Table 1. Differential cross-section for the energy distribution of Compton electrons (10). The table gives the number of Compton electrons per MeV interval at energy E, per electron of material per photon per cm^2. Multiply by 10^{-27} to obtain $\frac{d\sigma(E)}{dE}$ in cm^2 per electron.

E/E_{max}	Gamma Ray Energy (keV)				
	511	662	1173	1274	1332
	341	E_{max} 480	961	1061	1116
0	980	585	190	159	145
.1	935	552	188	155	141
.2	850	520	177	150	136
.3	790	490	173	146	134
.4	738	465	166	143	130
.5	698	445	166	143	131
.55	680	436	167	145	133
.60	670	435	168	146	134
.65	685	444	173	150	138
.70	700	458	182	158	146
.75	730	482	195	170	157
.80	800	530	214	186	173
.85	900	594	214	186	173
.90	1050	705	293	259	241
.95	1290	870	382	339	314
1.00	1630	1130	580	490	458

Table 2. Theoretical Compton distribution in the Cs^{137} spectrum.

E/E_{max}	E(keV)	Channel Number	Cross-section x 10^{-27}	Theoretical Counts
0	0	-36	585	28400
.1	48	-16	552	26800
.2	96	3	520	24700
.3	144	22	490	23800
.4	192	42	465	22600
.5	240	61	445	21600
.55	264	71	436	21150
.60	288	81	435	21100
.65	312	90	444	21500
.70	336	100	458	22200
.75	360	110	482	23400
.80	384	120	530	25200
.85	408	129	594	28800
.90	432	139	705	34200
.95	456	149	870	42200
1.00	480	158	1130	54600

EXPLANATION OF PLATE VII

A plot of the full energy peak-to-total ratio versus gamma ray energy for the detector used in this experiment. The dashed line is the ratio of the photo-electric cross-section to the total cross-section.

PLATE VII

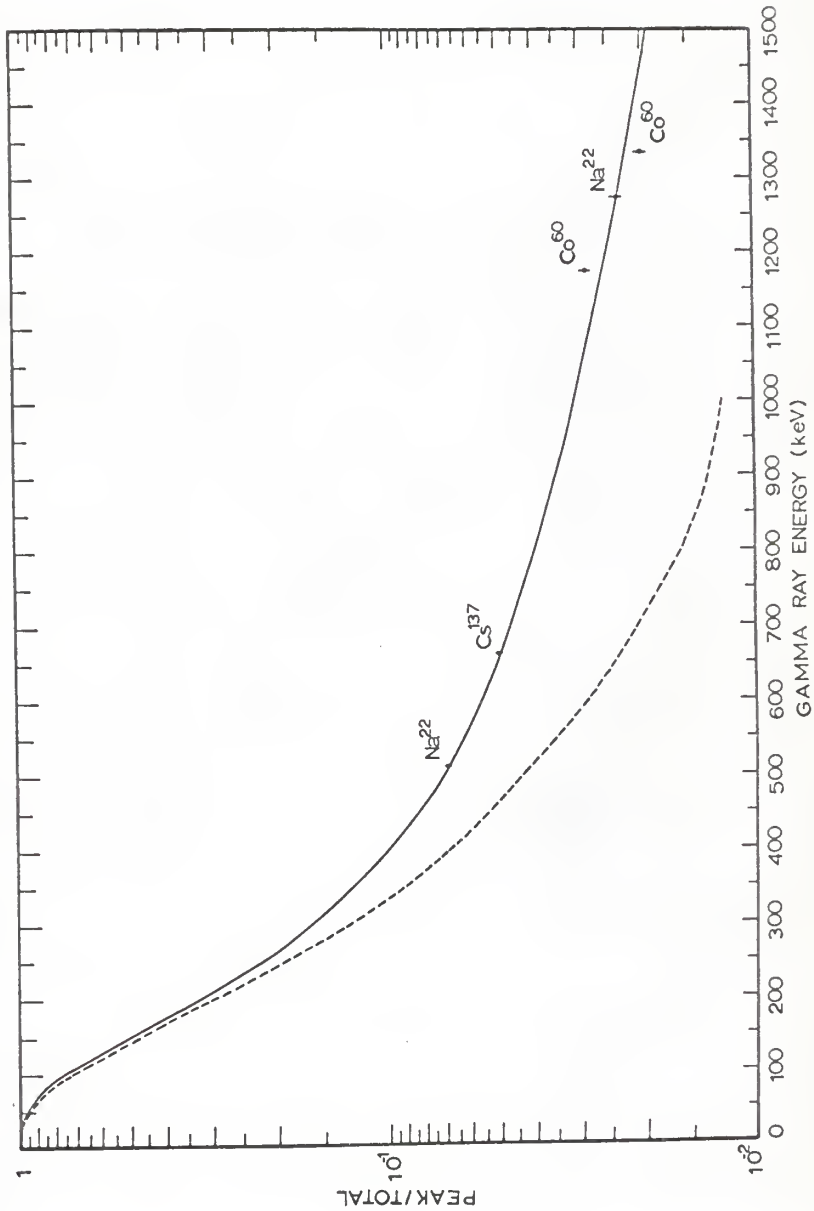
PEAK/TOTAL
1
10^{-1}
10^{-2}
0
100
200
300
400
500
600
700
800
900
1000
1100
1200
1300
1400
1500
GAMMA RAY ENERGY (keV)
Na^{22}
Cs^{137}
Co^{60}
Na^{22}
Co^{60}

the ratio of the photoelectric cross-section to the total cross-section.

The detection efficiency is defined as the number of gamma-rays interacting with the detector to the number of gamma-rays emitted from the source which entered the detector.

The geometry of the source and the detector is shown in Plate VIII.

For a point source at a distance "h" away from the face of the detector which is a cylinder with radius "r", thickness "t" and total attenuation coefficient "$\mu(E)$", the efficiency "e(E) at an energy "E" is

$$e(E) = \frac{1}{1 - \cos\theta}\left\{\int_0^{\Phi}\left[1 - e^{-\frac{\mu(E)t}{\cos\theta}}\right]\sin\theta d\theta + \right.$$

$$\left.\int_{\Phi}^{\theta}\left[1 - e^{-\mu(E)\left(\frac{r}{\sin\theta} - \frac{h}{\cos\theta}\right)}\right]\sin\theta d\theta\right\}$$

where $\theta = \tan^{-1}\frac{r}{h}$ and $\Phi = \tan^{-1}\frac{r}{h + t}$.

This expression must be corrected for every absorber used between the source and detector. Thus

$$e'(E) = e(E)\exp\left[-\Sigma\mu_i(E)t_i\right]$$

where $\mu_i(E)$ is the total attenuation coefficient and t_i is the thickness for the ith absorber.

The detection efficiency was computed on the Kansas State University's IBM 1401-1410 Computer. The program for this calculation was written by Agin (11).

EXPLANATION OF PLATE VIII

Geometry used for the calculation of detector efficiency.

PLATE VIII

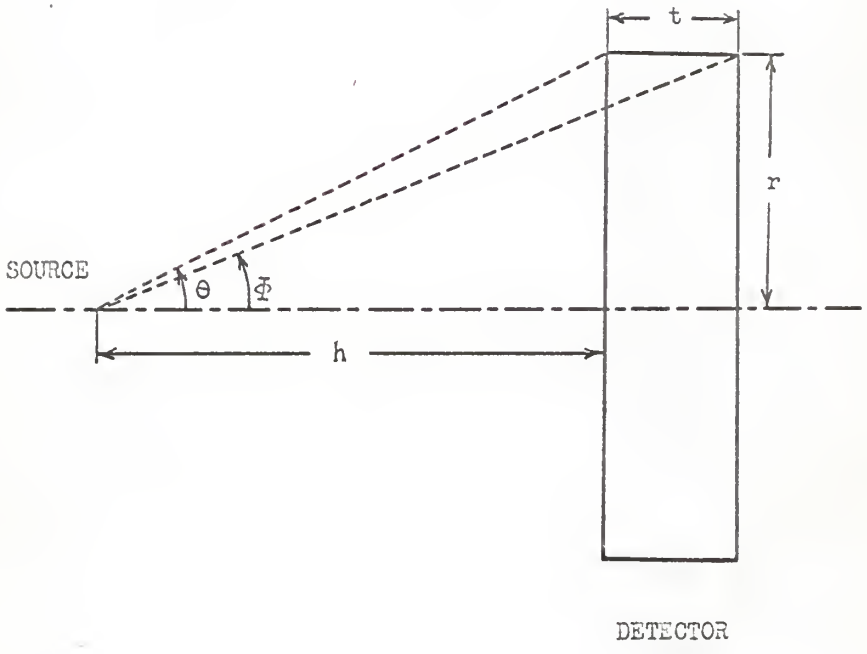

Radius of the detector: r = 1.6 cm

Thickness of the detector: t = 0.5 cm

Distance between the source and the face of the detector:

(a) For high energy spectra
h = 7.47 cm

(b) For low energy spectra
h = 18.47 cm

DETERMINATION OF RELATIVE INTENSITIES

The areas under the full-energy peaks were obtained from the differential pulse height distribution of gamma-rays in the decay of W^{187} by summing the counts per channel over the peak areas, and subtracting an estimated Compton background. These quantities were the "raw data". The correct data were then obtained by multiplying the raw data by appropriate correction factors for detection efficiency and peak-to-total ratio. The correction factors were the reciprocals of the detection efficiency and the peak-to-total ratio, respectively. The intensity data were normalized to the 479 keV gamma-ray which is 100 in intensity, by definition.

Several gamma ray spectra like the ones shown in Plates IV and V, were used to calculate the gamma-ray intensities of W^{187}. Table III shows the raw data and the corrections used to determine W^{187} gamma ray intensities. Comparison of the relative intensities determined in this experiment with the previously measured intensities is shown in Table IV.

Table 3. The raw data and the corrections used to determine W^{187} gamma ray intensities.

Gamma-Ray Energy	Peak-to-Total Ratio	Efficiency	Total Corr. Factor	Raw Counts (%error)	Correct Counts
Low Energy					
56	.955	.75	1.822	1,420,000 (2.82)	2,587,240
67	.92	.65	1.652	1,460,000 (2.06)	2.411,920
134	.600	.44	3.8	440,000 (6.97)	1,672,000
479	.076	.176	74.76	52,000 (1.93)	3,887,520
511	.0695	.17	84.63	880 (9.1)	74,474
551	.0633	.166	95.17	8,590 (.583)	817,510
618	.0546	.158	115.9	1,070 (5.61)	124,013
625	.0538	.157	118.4	8,500 (5.88)	1,006,400
High Energy					
479	.076	.14	93.99	475,000 (.842)	44,645,250
511	.0695	.1375	104.65	6,200 (9.68)	648,830
551	.0633	.135	117.01	72,000 (2.78)	8,424,720
618	.0546	.131	139.82	83,000 (.603)	11,605,060
625	.0538	.13	142.97	6,900 (4.35)	986,493
682	.0482	.126	164.67	278,000 (1.08)	45,778,260
745	.0435	.123	186.9	2,260 (2.66)	422,394
773	.0419	.122	195.63	32,800 (.915)	6,416,664
864	.037	.117	231.0	2,400 (4.16)	554,400
880	.036	.1155	240.5	900 (5.56)	216,450

Total correction factor is the reciprocal of the product of the peak-to-total ratio and the detection efficiency.

Table 4. Relative Intensities of Gamma Rays Emitted in the Decay of W^{187}.

Gamma Ray Energy(keV)	Dzhelepov et al.(2)	Gallagher et al.(3)	Arns et al. (4)	Michaelis (5)	Sébille et al.(6)	Present
72	——	48.5±1.9	65.7±13.1	56 ±8	——	44 ±3
134	——	39.3±1.2	47.2± 4.7	45 ±5	——	35 ±1
479	100	100	100	100	100 ±10	100
511	——	2.6± .2	——	⩽3.5	2.5± .8	1.7±.05
551	22.5±1.7	21.2± .7	28.7± 3	28.4±1.5	23 ±2	20.8±.2
618	31.2±2.5	26 ±1	38.9± 4	27.9±1.6	28 ±3	25.8±.3
625	——	4.3± .2	.85±.4	4.7± .9	5.5±1.1	4.0±.5
682	119 ±7	116 ±5	134 ± 7	110 ±6	123	103 ±2
745	——	——	——	——	.95±.1	.95±.03
773	22.2±1.5	16.2± .8	20.3± 2	17.6±1.6	19 ±2	14.4 ±.3
864	1.4± .3	1.54±.25	3.5± .4	2.0± .6	1.5± .2	1.24±.06
880	1.1± .3	——	——	——	.7± .2	.49±.03

CONCLUSION

Twelve gamma-rays in W^{187} decay were completely or partially resolved. The energies of these gamma-rays are 72, 134, 479, 511, 551, 618, 625, 682, 745, 773, 864, and 880 keV, and their relative intensities are 44, 35, 100, 1.7, 20.8, 25.8, 4, 103, 0.95, 14.4, 1.24, and 0.49 respectively.

The relative intensities of the 479, 511, 551, 618, 625, 682, 745, 773, 864, and 880 keV gamma-rays are in good agreement with those of Sébille (6). However, statistical accuracy has been improved in general by a factor of ten.

The intensities of the 72 and 134 keV gamma rays had not been previously studied with a semiconductor detector. The presently measured intensities of these two gamma-rays are in good agreement with the measurement of Gallagher (3).

Previously reported gamma-rays (3) 96, 107, 114, 206, 239, and 246 keV are not seen in the present measurement. However, their quoted intensities are smaller than that of the 880 keV gamma-rays. If present, these gamma-rays have intensities smaller than that of the 880 keV gamma-ray. Most of these gamma-rays would have their full energy peaks in the region of the strong Compton and backscatter distributions resulted from the higher energy gamma-rays. Thus, they have been masked to a certain extent. Since all of these gamma-rays are low in energy, they may have large conversion coefficients. The best way to measure their intensities would be the study of the interal conversion electron spectrum in a beta ray spectrometer.

ACKNOWLEDGEMENT

The author wishes to express his gratitude to Dr. C. E. Mandeville and Dr. V. R. Potnis for their support and guidance throughout the work. The author also expresses appreciation to Gary P. Agin for help with the computer programming. This work was supported in part by the U. S. Atomic Energy Commission.

BIBLIOGRAPHY

1. Dubey, V. S., C. E. Mandeville, A. Mukerji, and V. R. Potnis. Phys. Rev. 106, 785 (1957).

2. Dzhelepov, B. S., V. L. Rumiantsev, Ju. V. Kholnov, and G. E. Shchukin, Izv. Ak. Nauk. S. S. S. R., 24, no. 3, (1960).

3. Gallagher, C. J. Jr., W. F. Edwards, and G. Manning, Nucl. Phys., 19, 18 (1960).

4. Arns, R. G., and M. L. Wiedenbeck, Nucl. Phys., 19, 634 (1960).

5. Michaelis, W., Nucl. Phys., 48, 422 (1963).

6. Sébille, C., F. Widemann, R. Henck, L. Stab, and P. Siffert, Compt. Rend. 260, 3926 (1965).

7. Evans, R. D. The Atomic Nucleus, (McGraw-Hill Book Company, Inc., New York, 1955), Chap. 23-25.
   Arya, A. P. Fundamentals of Nuclear Physics, (Allyn and Bacon, Inc., Boston, 1966), Chap. 9.
   Seigbahn, K. Beta- and Gamma-ray Spectroscopy, (Interscience Publishers, New York, 1955), Chap. 2.

8. Heath, R. L. U. S. Atomic Energy Commission Reports, IDO-16880-1, (1964).

9. Goulding, F. S., Nucl. Instr., 43, 1 (1966).

10. Johns, H. E., D. V. Cormack, S. A. Denesuk, and G. F. Whitmore, Can. J. Phys. 30, 556 (1952).

11. Agin, G. P., M. S. Thesis, Kansas State University, (1967).

RELATIVE INTENSITIES OF GAMMA RAYS IN BETA DECAY OF W 187

by

NAI CHENG CHAO

Diploma, Taiwan Provincial Taipei Institute of Technology, 1962

AN ABSTRACT OF A MASTER'S THESIS

submitted in partial fulfillment of the

requirements for the degree

MASTER OF SCIENCE

Department of Physics

KANSAS STATE UNIVERSITY
Manhattan, Kansas

1967

The relative intensities of gamma-rays emitted from W^{187} (T 1/2 = 24 h) have been measured with a lithium-drifted germanium detector. This detector has an active area of 8 cm^2 and a depletion depth of 5 mm. This high energy resolution Ge(Li) detector, incorporated with a 4096-channel multiparameter pulse-height analyzer, provides an accurate method of investigating the decay of W^{187}.

The full energy peak-to-total ratio and the efficiency of the Ge(Li) detector, as functions of energy have been experimentally measured. These detector parameters are needed for determination of the relative intensities of the gamma-rays.

Twelve gamma-rays in W^{187} decay were completely or partially resolved. The energies of these gamma-rays are 72, 134, 479, 511, 551, 618, 625, 682, 745, 773, 864, and 880 keV, and their relative intensities are 44, 35, 100, 1.7, 20.8, 25.8, 4, 103, 0.95, 14.4, 1.24, and 0.49 respectively. The relative intensities of the 479, 511, 551, 618, 625, 682, 745, 773, 864, and 880 keV gamma-rays are in good agreement with those of Sébille. However, statistical accuracy of the intensities measurement has been improved in general by a factor of ten. The intensities of the 72 and 134 keV gamma-rays have not been studied with semiconductor before. The intensities of these two-gamma-rays in this work show good agreement with those of Gallagher.